Effect of temperature on electron attachment to and negative ion states of CCl_2F_2

Yicheng Wang,[a] Loucas G. Christophorou,[b] and Joel K. Verbrugge
National Institute of Standards and Technology, Electricity Division, Electronics and Electrical Engineering Laboratory, Gaithersburg, Maryland 20899-0001

(Received 19 June 1998; accepted 14 August 1998)

The effect of temperature on electron attachment to dichlorodifluoromethane (CCl_2F_2) has been investigated for temperatures up to 500 K and for mean-electron energies from thermal to 1.0 eV using an electron swarm method. The measurements were made in mixtures of CCl_2F_2 with nitrogen. The electron attachment rate constant increases with temperature over the entire temperature and mean-electron energy range investigated. The variation of the thermal value of the electron attachment rate constant with temperature compares well with earlier measurements of this quantity and shows an increase by a factor of 10 when the temperature is raised from 300 to 500 K. From a comparison of published data on the electron affinity, electron attachment using the swarm method, electron attachment using the electron beam method, electron scattering, electron transmission, indirect electron scattering, and related calculations, the lowest negative ion states of CCl_2F_2 have been identified with average positions as follows: $a_1(\text{C–Cl}\sigma^*)$ at $+0.4$ eV and -0.9 eV, $b_2(\text{C–Cl}\sigma^*)$ at -2.5 eV, $a_1(\text{C–F}\sigma^*)$ at -3.5 eV, and $b_1(\text{C–F}\sigma^*)$ at -6.2 eV; an electron-excited Feshbach resonance is also indicated at -8.9 eV. © *1998 American Institute of Physics.* [S0021-9606(98)02043-1]

I. INTRODUCTION

There have been a number of studies dealing with the interactions of dichlorodifluoromethane (CCl_2F_2) with low-energy electrons. These have recently been reviewed by Christophorou *et al.*[1] In this paper we report on two aspects of low-energy (<10 eV) electron interaction processes in CCl_2F_2: (1) The measurement of the temperature dependence of the total electron attachment rate constant for CCl_2F_2 in the mean electron energy range from 0.04 to 1.00 eV and the temperature range from 300 to 500 K. These measurements were made using a pulsed Townsend swarm technique[2] and a new wave form analysis method which improved data quality. (2) The number and energy position of the negative ion states of the CCl_2F_2 molecule below ~ 10 eV. This knowledge is obtained by a synthesis of published data from experiments and calculations.

II. EXPERIMENTAL METHOD

The experimental method employed here is a pulsed Townsend technique[2] whereby electron swarms are photoelectrically produced using a 5 ns, frequency quadrupled (266 nm) Nd:YAG laser. A schematic diagram showing its operating principle is given in Fig. 1. The two parallel electrodes are circular stainless steel disks with a diameter of 6.2 cm. They are separated by a distance, d, of 1.664 cm and are contained in a cubic stainless steel vacuum chamber. The laser beam enters the chamber through a sapphire window and is focused through a small hole (~ 0.6 mm diam) in the center of the anode electrode before striking the cathode electrode, generating a photoelectron pulse which quickly reaches a steady state and drifts toward the anode under the influence of the applied uniform electric field, E. The current induced by the motion of this electron swarm and the negative ions which are formed by attachment in the drift (interelectrode) region is integrated by the RC ($R=100$ GΩ and $C\sim 50$ pF) circuit in front of a high-impedance unity-gain buffer amplifier with a slew rate of 0.22 V/ns. The output voltage of the amplifier is then digitized with a LeCroy 9420 digital oscilloscope (Certain commercial equipment, instruments, or materials are identified in this paper to foster understanding. Such identification does not imply recommendation or endorsement by the National Institute of Standards and Technology, nor does it imply that the materials or equipment identified are necessarily the best available for the purpose.) which has a resolution of eight bits and a maximum sample rate of 10^8 samples/s. To minimize the influence of the alternating current (ac) line noise, laser pulses are synchronized with the zero crossings of the line frequency. The synchronization scheme allows subtraction of the line noise and thus improvement in data quality.

The vacuum chamber is enclosed in a fiberglass heating mantle. The heating power to the mantle is controlled with an Autotune Temperature Controller (CN9000A) made by Omega, achieving a temperature stability within 1 °C. The temperature uniformity of the chamber is monitored with multiple thermocouples around the chamber and is constant to within 1 °C. The experiments were performed using N_2 (quoted purity 99.999%) and CCl_2F_2 (quoted purity 99.9%) purchased from Matheson Gas Products. Before use, the N_2 gas was cooled to liquid nitrogen temperature to condense

[a]Electronic mail: Yicheng.Wang@nist.gov
[b]Electronic mail: loucas.christophorou@nist.gov

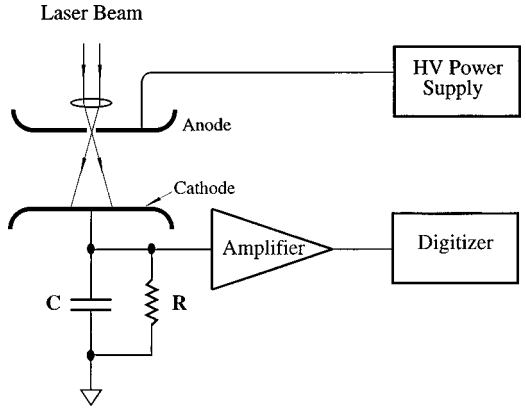

FIG. 1. Schematic diagram of the pulsed Townsend method used in the present study (see text).

impurities, especially H_2O. The N_2 vapor was extracted just above the boiling point. The CCl_2F_2 gas was also purified by a number of freeze–pump–thaw cycles to remove air and other possible impurities. In the experiments conducted in this work, the N_2 buffer gas pressure was varied from 75.3 to 127 kPa and the partial pressure of CCl_2F_2 was 5.12, 1.63, and 0.449 Pa for data taken at temperatures of 298, 400, and 500 K, respectively. The total pressures and the mixture ratios were measured using two temperature-controlled, high-accuracy capacitance manometers. The estimated measurement uncertainty for the total pressure, the mixture ratio, and E/N is less than $\pm 1\%$.

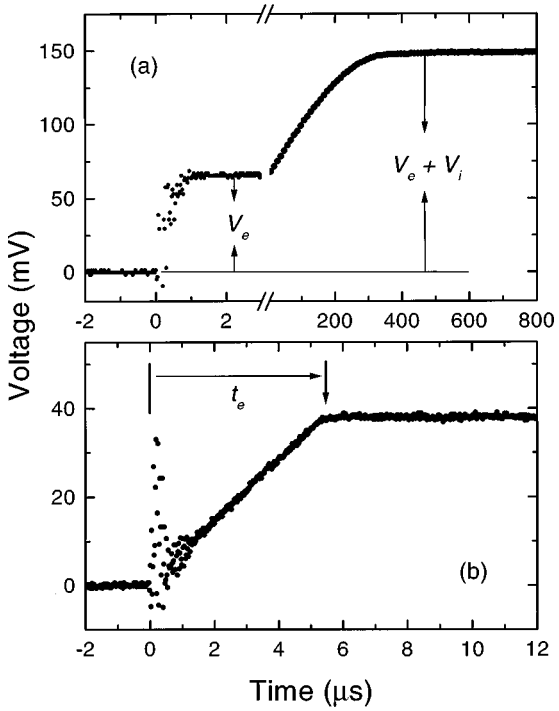

FIG. 2. Typical voltage wave forms at room temperature. (a) For a mixture of CCl_2F_2 and N_2 (attaching gas to buffer gas density ratio $=6.8\times10^{-5}$; note the change in the time scale for V_e and V_e+V_i) and an E/N value of 0.33 Td. (b) For pure N_2 at $E/N=0.29$ Td (the signal ''peak'' at the origin is due to the laser pulse) (see text).

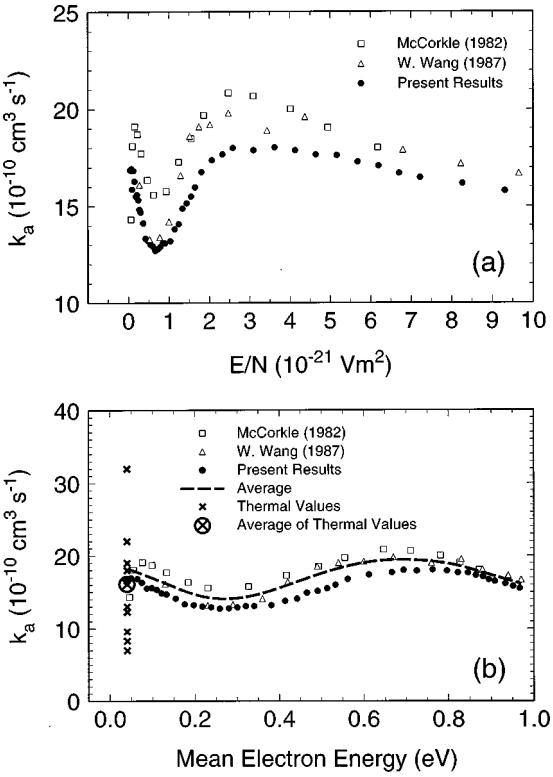

FIG. 3. Total electron attachment rate constant k_a for CCl_2F_2 measured at room temperature in mixtures with N_2. (a) as a function of E/N (□, Ref. 3; △, Ref. 4; ●, present), and (b) as a function of the mean-electron energy. Also shown in the (b) are values of k_a, measured at only thermal energy.

Two typical voltage wave forms that were acquired at room temperature are shown in Fig. 2. The wave form in Fig. 2(a) was acquired in a $CCl_2F_2+N_2$ mixture (the ratio of CCl_2F_2 to N_2 was 6.8×10^{-5}, and the density-reduced electric field E/N was 0.33×10^{-17} V cm^2). The initial voltage step, V_e, which occurs in $t\approx1$ μs, is proportional to the number of electrons drifting across the gap without attachment. The plateau voltage, V_e+V_i, which is reached at $t\approx400$ μs, is proportional to the sum of the electrons and the negative ions crossing the gap. The electron attachment coefficient, η, is determined from

$$V_e/(V_e+V_i)=[1-\exp(-\eta d)]/(\eta d). \quad (1)$$

TABLE I. Values of the thermal electron attachment rate constant, $(k_a)_{th}$, for CCl_2F_2. Average value: $(16.1\pm7.2)\times10^{-10}$ cm^3 s^{-1}.

$(k_a)_{th}$(10^{-10} cm^3 s^{-1})	T (K)	Method	Reference
16.6	298	Electron swarm	Present
9.6	295	Electron swarm	5
13	298	Microwave conductivity	6
8.3	300	Electron cyclotron resonance	7
7	298	Electron cyclotron resonance	8
18	293	Electron cyclotron resonance	9
19	298	Electron swarm	10
12.3	298	Electron swarm	3 and 11
22	298	Electron swarm	12
32	300	Flowing afterflow	13 and 14
19	293	Flowing afterglow	15

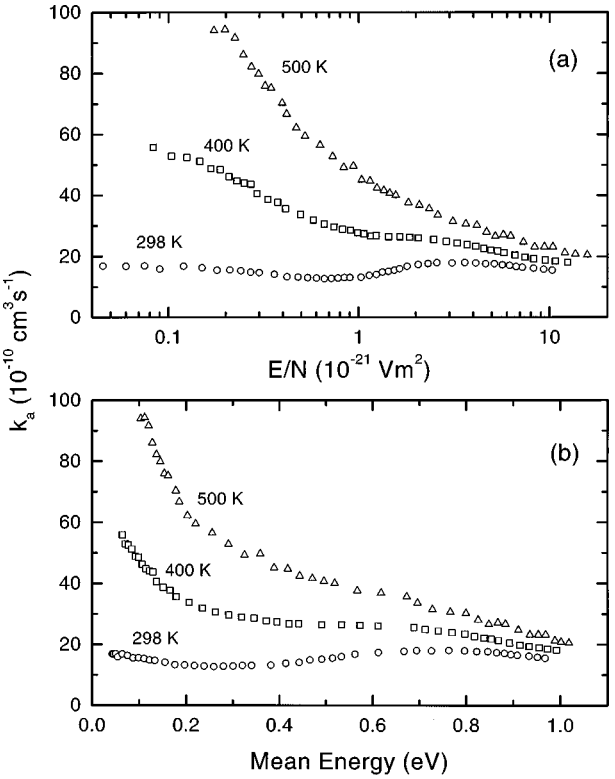

FIG. 4. Variation of the k_a of CCl_2F_2 with temperature. (a) $k_a(E/N)$, (b) $k_a(\langle\epsilon\rangle)$.

The digital oscilloscope used in the present work has a record length of 50 000 samples for each laser pulse, which allows recording of wave form details in multiple time scales. This capability of the present experiment of acquiring detailed data in multiple time scales allows more accurate determination of V_e and V_e+V_i and is an improvement over earlier data acquisition procedures which use the pulsed Townsend method.

The wave form shown in Fig. 2(b) was taken in pure N_2 at an E/N of 0.29×10^{-17} V cm^2 with the sample rate of the digital oscilloscope set to the maximum. The distinct break at $t=5.5$ μs is associated with the electron swarm transit time, t_e. The response time of the electronic system is shorter than 20 ns. The electron drift velocities, $w=d/t_e$, are determined from the occurrence time of this break, and have an estimated uncertainty of $\pm5\%$. The uncertainty is primarily due to determining the position of the break point and is determined from the standard deviation of the scatter observed in multiple runs for identical experimental conditions.

TABLE II. $(k_a)_{th}$ of CCl_2F_2 as a function of temperature.

$(k_a)_{th}$(10^{-10} cm^3 s^{-1})	T (K)	Reference
16.6	298	Present work
60	400	
<140	500	
<10	205	13 and 14
32	300	
160	455	
530	590	
19	293	15
140	467	
240	579	
420	777	

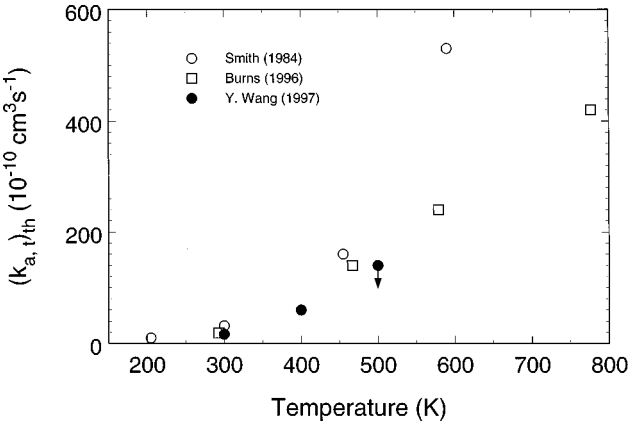

FIG. 5. Variation of the thermal value, $(k_a)_{th}$, of the total electron attachment rate constant for CCl_2F_2 with temperature. ●, present; ○, Refs. 13 and 14; □, Ref. 15. The arrow shown for one of the data points indicates that the value of $(k_a)_{th}$ is lower than shown.

The total electron attachment rate constant, k_a, is obtained from

$$k_a = w\,\eta/N_a, \tag{2}$$

where N_a is the number density of the electron attaching gas. The combined experimental uncertainty for k_a is approximately $\pm10\%$ for data acquired at 298 and 400 K. For the data acquired at 500 K, the uncertainty is approximately $\pm20\%$. The larger uncertainty at this higher temperature is related to possible thermal decomposition of CCl_2F_2.

III. TEMPERATURE DEPENDENCE OF THE ELECTRON ATTACHMENT RATE CONSTANT FOR CCl_2F_2

We measured the total electron attachment rate constant, k_a, for CCl_2F_2 as a function of E/N in nitrogen at room temperature (298), 400, and 500 K. In Fig. 3(a) are shown our room temperature measurements of k_a (E/N) along with two earlier room temperature measurements.[3,4] The variation between the data of the various groups is barely within the combined uncertainties which are about $\pm10\%$ for each experiment. The data in Fig. 3(a) are plotted in Fig. 3(b) as a function of the mean-electron energy, $\langle\epsilon\rangle$, calculated from the electron energy distribution functions in N_2 using a Boltzmann code. Also, there have been a number of earlier measurements of only the room temperature thermal value, $(k_a)_{th}$, of k_a. These are listed in Table I and are plotted in Fig. 3 along with their average, $(16.1\pm7.2)\times10^{-10}$ cm^3 s^{-1}.

Figure 4(a) shows the measured dependence of k_a (E/N) on temperature, and Fig. 4(b) shows the same data plotted as a function of mean-electron energy $\langle\epsilon\rangle$. The rate constant is seen to increase considerably with increasing temperature over the entire energy range from 0.04 to 1.0 eV. However, the lower the value of $\langle\epsilon\rangle$ the larger the temperature enhancement. This behavior is consistent with earlier findings on other compounds[16] and with the results of two recent elec-

TABLE III. Negative ion states of CCl_2F_2.

Energy (eV)	Method	Reference
0.4 ± 0.3	Potassium-atom beam technique	20
0.4	Multiple scattering X_α calculation	21 and 22
0.67	Quantum mechanical calculation	23
~0.0	Kr photoionization electron attachment technique	24
<-0.1	Swarm-unfolded total attachment cross	12
~ -0.18 (shoulder)	section using N_2 as the buffer gas	
−1.05		
−0.07	Swarm-unfolded total attachment cross	3
−0.30	section using N_2 as the buffer gas	
−0.93		
~0	Swarm-unfolded total attachment cross	25
−0.8	section using N_2 and Ar as buffer gases	
−3.8		
~0.0	Energies where the total attachment rate	4
~ -0.7	constant measured in N_2 and Ar buffer gases	
~ -3.5	shows maxima	
~0.0	Electron beam measurement of the total	26
~ -0.6	attachment cross section	
−3.5		
-0.55 (Cl^-)	Mass spectrometric study of dissociative	27–29
-0.65 (Cl_2^-)	attachment using a trochoidal monochromator	
-2.85 (FCl^-)		
-3.1 (F^-)		
-3.55 ($CFCl_2^-$)		
The energy dependence of the sum of all negative ions gives peaks at −0.6 eV and at −3.2 eV (Ref. 1)		
~0.0	Mass spectrometric study of dissociative	30
−0.3	attachment using a trochoidal monochromator	
−0.95		
−3.6		
-0.7 (Cl^-)	Ion cyclotron resonance study of dissociative attachment	31
-3.2 (F^-)		
-3.7 ($CFCl_2^-$)		
−1.0	Total electron scattering cross-section	32
−2.6	measurements	
−4.0		
−5.9		
−1.2	Estimates[a] of resonance energies determined	33
−3.4	from electron scattering experiments	
−4.6		
−6.4		
−0.8	Quantum mechanical calculation[a]	33
−3.1		
−5.1		
−6.7		
−0.98	Vertical electron affinity values determined	34
−2.35	by electron transmission spectroscopy	
−3.88		
−1.0	Maxima in the total indirect inelastic electron	Analysis by
−2.5	scattering cross section	Christophorou *et al.* (Ref. 1)
−4.0		based on the work of
−6.0		Mann and Linder (Ref. 35)
−9.0		

[a]From fig. 5 of Ref. 33.

tron beam studies[17,18] on the temperature dependence of the production of Cl^- from CCl_2F_2. No other measurements have been made at temperatures higher than ambient at energies higher than thermal. However, there have been two measurements[14,15] of the *thermal* value, $(k_a)_{th}$, of the total electron attachment rate constant of CCl_2F_2 as a function of gas temperature. These data are listed in Table II and are compared with the present results in Fig. 5. While there is considerable disagreement in the absolute value of $(k_a)_{th}$ as measured by the various groups, the variation of $(k_a)_{th}$ with temperature is rather consistent. The strong effect of internal vibrational energy on the dissociative attachment of thermal electrons to the CCl_2F_2 molecule is manifested at even lower temperatures than shown in Table II as recent measurements of the $(k_a)_{th}$ for supersonically cooled CCl_2F_2 in the temperature range from 48 to 170 K have shown.[19]

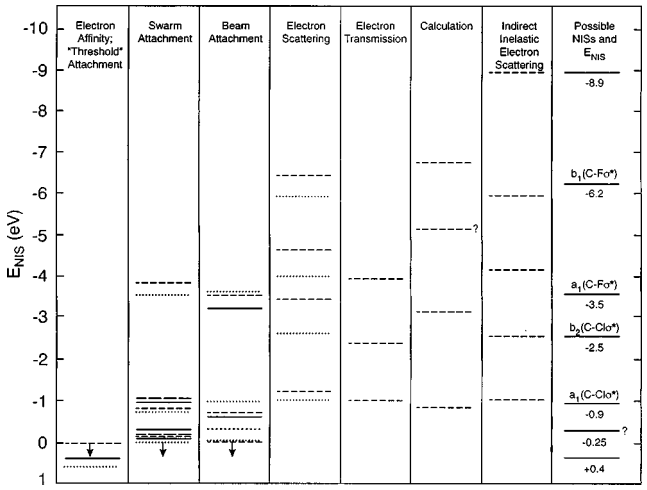

FIG. 6. Energy positions, E_{NIS}, of the negative ion states of CCl_2F_2 below ~10 eV as obtained by various methods. Column 1: — — —[threshold attachment technique (Ref. 24)]; _____ [potassium–atom charge–exchange collision technique (Ref. 20), calculation (Refs. 21 and 22); ....., calculation (Ref. 23)]. Column 2: Electron swarm attachment techniques: — — —, Ref. 25; ....., Ref. 4; — — —; Ref. 12; ____, Ref. 3, present. Column 3; Electron beam attachment techniques: — — —, Ref. 26; ____, Ref. 27 (peaks in the sum of all negative ions, see Table III); ..., Ref. 30. Column 4: Electron scattering: ....., Ref. 32; — — —, Ref. 33. Column 5: Electron transmission: — — —, Ref. 34. Column 6: Calculation: — — —, Ref. 33. Column 7: Indirect inelastic electron scattering: — — —, Ref. 1. Column 8: Possible negative ion states and their energies and assignments. The arrows shown in columns 1, 2, and 3 indicate that the energies of these resonances as determined by the corresponding methods are lower than shown in the figure.

IV. NEGATIVE ION STATES OF CCl_2F_2

In an effort to identify the number of negative ion states of the CCl_2F_2 molecule below ~10 eV and their energies, we searched for information from various experimental and theoretical sources. Table III summarizes the information found in the literature from six different types of experimental methods: The heavy-atom collision technique,[20] the Kr photoionization electron attachment technique,[24] the swarm electron attachment technique,[3,4,12,25] electron beam/mass spectrometric techniques for electron attachment,[26–30] electron scattering,[31–33] and electron transmission.[34] Additionally, information obtained from a number of calculations,[21–23,33,34] and the recent analysis by Christophorou *et al.*[1] is also listed in Table III. The data in Table III are compared in Fig. 6. The adiabatic electron affinity, E.A., of CCl_2F_2 has been determined by Dispert and Lacmann[20] to be $0.4\ \mathrm{eV} \pm 0.3\ \mathrm{eV}$ using a potassium-atom beam to create $CCl_2F_2^-$ via electron transfer in binary potassium–CCl_2F_2 collisions. A multiple-scattering X_α (MSX_α) calculation[21,22] also gave a positive value for the E.A. of the CCl_2F_2 molecule equal to 0.4 eV. Similarly, a more recent quantum mechanical calculation[23] also gave a positive value for the adiabatic electron affinity of the CCl_2F_2 molecule equal to +0.67 eV.

In the last column of Fig. 6 are given the ''average'' positions of the negative ion states of CCl_2F_2 based on the data given in the figure. Clearly, on the basis of the present comparison of all the various data, there exist at least four negative states below the electronic excitation threshold of the CCl_2F_2 molecule whose average energy positions are: +0.4 and −0.9 eV (these two belong to the same state, see below), −2.5, −3.5, and −6.2 eV. Another resonance at −8.9 eV lies in the region of electronic excitation and most likely is associated with excited electronic states. The additional state indicated by some experiments at −0.25 eV is questionable; its existence is shown by two electron swarm studies and one electron beam study, but is absent from the cross section of another similar beam study. It may be associated with vibrationally excited molecules. The calculation of Underwood–Lemons *et al.*[33] located a state at −4.9 eV but most likely this should be associated with the −3.5 eV resonance since no experimental evidence exists for a resonance at this energy from any other source and since the calculation predicts four negative ion states which can be rationalized with other studies and molecular orbital assignments.

In an attempt to rationalize the positions of the negative ion states of CCl_2F_2 in the last column of Fig. 6 we note the following: (1) The calculations of Tossell[23] (see also Ref. 33) have shown profound geometrical changes between CCl_2F_2 and $CCl_2F_2^-$. (2) According to an *ab initio* SCF (self-consistent field) calculation on the neutral CCl_2F_2 molecule by Burrow *et al.*,[34] four valence-type resonances are expected below about 5 eV which can be ascribed, in increasing energetic order, to the unoccupied orbitals $a_1(\mathrm{C–Cl}\sigma^*)$, $b_2(\mathrm{C–Cl}\sigma^*)$, $a_1(\mathrm{C–F}\sigma^*)$, and $b_1(\mathrm{C–F}\sigma^*)$. Burrow *et al.* have ascribed the resonances they detected in an electron transmission experiment at 1.0, 2.5, and 4.0 eV to the lowest three of these molecular orbitals. (3) Mann and Linder[35] measured the energy-loss spectra of CCl_2F_2 for electrons having initial energies equal to 1.0, 2.4, 4.0, and 6.0 eV, i.e., roughly equal to the energy positions of the observed four negative ion resonances of CCl_2F_2. Their results have shown

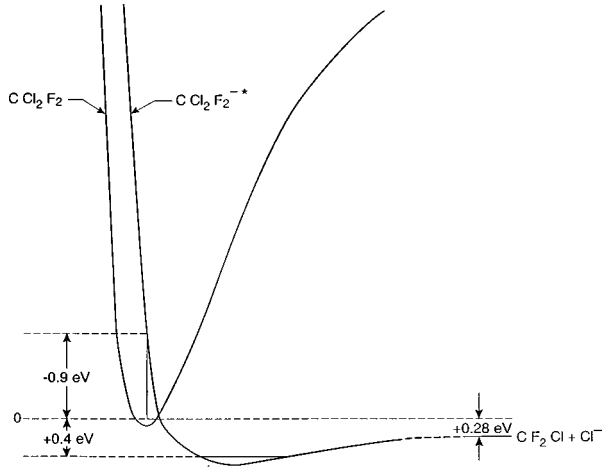

FIG. 7. Schematic potential-energy curves for $CF_2Cl–Cl$ and the lowest negative ion state of $CCl_2F_2^{-*}$ consistent with the (adiabatic) positive (+0.4 eV) electron affinity of CCl_2F_2, the vertical electron affinity (−0.9 eV) of the lowest negative ion state of CCl_2F_2, and the observation that the dissociative electron attachment cross section rises steeply as the electron energy decreases towards zero (Ref. 1). The asymptotic limit CF_2Cl+Cl^- lies 0.28 eV below the 0.0 eV level taken to be at the $v=0$ level of the $CClF_2–Cl$ symmetric stretch vibration ν_3, using a value of 3.33 eV for the $CClF_2–Cl$ dissociation energy and a value of 3.61 eV for the electron affinity of the Cl atom (see text).

that for 1.0 eV, the most prominent energy loss is the excitation of the ν_3 vibration. This is consistent with the (C–Clσ^*) character of the a_1(C–Clσ^*) resonance at 1.0 eV. Consistent with this assignment of the 1.0 eV resonance are also the data on dissociative electron attachment around this energy,[29–31] both for the production of Cl^- involving the breaking of the C–Cl bond and for the production of Cl_2^- involving the C–Cl_2 dissociation. Additionally, the study of Mann and Linder showed that in the a_1(C–Fσ^*) resonance at 4.0 eV, the excitation of $v_{1,6}$ is the dominant process. This is consistent with the (C–Fσ^*) character of this resonance. The a_1(C–Fσ^*) resonance at 4.0 eV is also the appropriate precursor of the group of the fragment negative ions observed[29–31] at 3.5 eV (the position of the resonance apparently is shifted downward by about 0.5 eV in the dissociative attachment channel in comparison to the scattering channel due to the competition between dissociation and autoionization). The dominant fragment anion at this energy is F^- in accordance with the (C–Fσ^*) character of this resonance. Interestingly, the b_2(C–Clσ^*) resonance at 2.5 eV does not decay via dissociative attachment since none of the electron attachment studies has shown a peak at this energy. Peculiarly, this resonance shows up only in the vibrational excitation channel.[35] (4) The data in Figs. 3 and 4 clearly show that the CCl_2F_2 molecule attaches electrons with energies less than 1 eV, and that below ~0.3 eV the attachment rate constant increases with decreasing energy toward thermal energies for all temperatures investigated.

In view of the findings mentioned above, it may be concluded that the potential-energy surface of the lowest negative ion state of CCl_2F_2 has a minimum at about 0.4 eV below that of the neutral molecule, and that it rises steeply in the Franck–Condon region to account for the vertical attachment energy at −0.9 eV. The potential-energy curve for this state is shown schematically in Fig. 7. This state, then, accounts for both the positive E. A. (+0.4 eV) and for the first observed vertical attachment energy at −0.9 eV and is assigned to a_1(C–Clσ^*). The electron attachment reactions below about 1 eV predominantly lead to dissociation producing Cl^-. Since the CF_2Cl–Cl bond dissociation energy [3.3 eV±0.2 eV (Ref. 20); 3.58 eV (Ref. 27); 3.1 eV (Ref. 36)] is smaller than the electron affinity (3.61 eV, Ref. 37) of the Cl atom, the reaction

$$CCl_2F_2 + e \rightarrow CClF_2 + Cl^-, \tag{3}$$

is exoergic. The energy position of this negative ion state would make the dissociative attachment process highly temperature dependent i.e., the rate constant is expected to increase with increasing temperature, thus accounting for the observed behavior. The higher negative ion states at −2.5, −3.5, and −6.2 eV, are identified with the assignments of Burrow *et al.*, namely, the b_2(C–Clσ^*), a_1(C–Fσ^*), and b_1(C–Fσ^*) unoccupied orbitals, respectively.

V. CONCLUSIONS

The main conclusions of the present work are:

(1) The rate constant for electron attachment to the CCl_2F_2 molecule increases with increasing temperature from 300 to 500 K over the entire mean-electron energy range from 0.04 to 1.0 eV investigated. The lower the value of the mean-electron energy, the larger the temperature enhancement. At thermal energies the electron attachment rate constant shows an increase by a factor of 10 when the temperature is raised from 300 to 500 K. The measurements also show that the attachment rate constant increases below about 0.3 eV as the mean-electron energy approaches its thermal value indicating that the potential-energy surface for the lowest CCl_2F_2 negative ion state crosses that of the neutral molecule near its minimum.

(2) The lowest negative ion states of CCl_2F_2 have been identified with average positions as follows: a_1(C–Clσ^*) at +0.4 eV and −0.9 eV, b_2(C–Clσ^*) at −2.5 eV, a_1(C–Fσ^*) at −3.5 eV, and b_1(C–Fσ^*) at −6.2 eV.

(3) In view of (1) and (2), it may be concluded also that the potential-energy surface of the lowest [a_1(C–Clσ^*)] negative ion state of CCl_2F_2 has a minimum at about 0.4 eV below that of the neutral molecule, and that it rises steeply in the Franck–Condon region to account for the vertical attachment energy at −0.9 eV. This state, then, accounts for both the positive E. A. (+0.4 eV) and for the first observed vertical attachment energy at −0.9 eV.

[1] L. G. Christophorou, J. K. Olthoff, and Y. Wang, J. Phys. Chem. Ref. Data **26**, 1205 (1997).
[2] S. R. Hunter, J. G. Carter, and L. G. Christophorou, J. Appl. Phys. **60**, 24 (1986).
[3] D. L. McCorkle, A. A. Christodoulides, L. G. Christophorou, and I. Szamrej, J. Chem. Phys. **72**, 4049 (1980).
[4] W. C. Wang and L. C. Lee, IEEE Trans. Plasma Sci. **PS-15**, 460 (1987).
[5] I. Szamrej, W. Tchorzewska, H. Kosc, and M. Forys, Radiat. Phys. Chem. **47**, 269 (1996).
[6] K. M. Bansal and R. W. Fessenden, J. Chem. Phys. **59**, 1760 (1973).
[7] K. G. Mothes, E. Schultes, and R. N. Schindler, J. Phys. Chem. **76**, 3758 (1972).
[8] R. Schumacher, H.-R. Sprünken, A. A. Christodoulides, and R. N. Schindler, J. Phys. Chem. **82**, 2248 (1778).
[9] C. J. Marotta, C. Tsai, and D. L. McFadden, J. Chem. Phys. **91**, 2194 (1989).
[10] L. G. Christophorou, Chem. Rev. **76**, 409 (1976).
[11] L. G. Christophorou, R. A. Mathis, D. R. James, and D. L. McCorkle, J. Phys. D **14**, 1889 (1981).
[12] L. G. Christophorou, D. L. McCorkle, and D. Pittman, J. Chem. Phys. **60**, 1183 (1974).
[13] D. Smith and P. Spanel, Adv. At., Mol., Opt. Phys. **32**, 307 (1994).
[14] D. Smith, N. G. Adams, and E. Alge, J. Phys. B **17**, 461 (1984).
[15] S. J. Burns, J. M. Matthews, and D. L. McFadden, J. Phys. Chem. **100**, 19436 (1996).
[16] L. G. Christophorou, L. A. Pinnaduwage, and P. G. Datskos, in *Linking the Gaseous and the Condensed Phases of Matter*, edited by L. G. Christophorou, E. Illenberger, and W. F. Schmidt (Plenum, New York, 1994), p. 415.
[17] A. Kiendler, S. Matejcik, J. D. Skalny, A. Stamatovic, and T. D. Märk, J. Phys. B **29**, 6217 (1996).
[18] I. Hahndorf and E. Illenberger, Int. J. Mass Spectrom. Ion Processes **167/168**, 87 (1997).
[19] J. L. Le Garrec, O. Sidko, J. L. Queffelec, S. Hamon, J. B. A. Mitchell, and B. R. Rowe, J. Chem. Phys. **107**, 54 (1997).
[20] H. Dispert and K. Lacmann, Int. J. Mass Spectrom. Ion Phys. **28**, 49 (1978).
[21] H. J. T. Preston and J. J. Kaufman, Chem. Phys. Lett. **50**, 157 (1977).
[22] J. J. Kaufman, H. E. Popkie, and H. J. T. Preston, Int. J. Quantum Chem. **11**, 1005 (1977).
[23] J. A. Tossell, quoted in Ref. 1.
[24] A. Chutjian and S. H. Alajajian, J. Phys. B **20**, 839 (1987).
[25] Z. Lj. Petrovic, W. C. Wang, and L. C. Lee, J. Chem. Phys. **90**, 3145 (1989).

[26] V. M. Pejcev, M. V. Kurepa, and I. M. Cadez, Chem. Phys. Lett. **63**, 301 (1979).
[27] E. Illenberger, H.-U. Scheunemann, and H. Baumgärtel, Chem. Phys. **37**, 21 (1979).
[28] E. Illenberger, Ber. Bunsenges. Phys. Chem. **86**, 252 (1982).
[29] T. Oster, A. Kühn, and E. Illenberger, Int. J. Mass Spectrom. Ion Processes **89**, 1 (1989).
[30] T. Underwood-Lemons, T. J. Gergel, and J. H. Moore, J. Chem. Phys. **102**, 119 (1995).
[31] G. J. Verhaart, W. J. van der Hart, and H. H. Brongersma, J. Chem. Phys. **34**, 161 (1978).
[32] R. K. Jones, J. Chem. Phys. **84**, 813 (1986).
[33] T. Underwood-Lemons, D. C. Winkler, J. A. Tossell, and J. H. Moore, J. Chem. Phys. **100**, 9117 (1994).
[34] P. D. Burrow, A. Modelli, N. S. Chiu, and K. D. Jordan, J. Chem. Phys. **77**, 2699 (1982).
[35] A. Mann and F. Linder, J. Phys. B **25**, 1633 (1992).
[36] W. E. Wentworth, R. George, and H. Keith, J. Chem. Phys. **51**, 1791 (1969).
[37] A. A. Christodoulides, D. L. McCorkle, and L. G. Christophorou, in *Electron Molecule Interactions and their Applications*, edited by L. G. Christophorou (Academic, New York, 1984), Vol. 2, Chap. 6.